



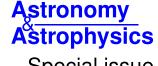
AperTO - Archivio Istituzionale Open Access dell'Università di Torino

## **Chemical cartography of the Milky Way**

inis is the author's manuscript	
Original Citation:	
Availability:	
This version is available http://hdl.handle.net/2318/1948498	since 2023-12-19T15:18:11Z
Published version:	
DOI:10.1051/0004-6361/202243511	
Terms of use:	
Open Access  Anyone can freely access the full text of works made available as 'under a Creative Commons license can be used according to the te of all other works requires consent of the right holder (author or puprotection by the applicable law.	erms and conditions of said license. Use

(Article begins on next page)

Gaia Data Release 3



# Special issue

# Gaia Data Release 3

# Chemical cartography of the Milky Way

```
Gaia Collaboration: A. Recio-Blanco<sup>1,★</sup>, G. Kordopatis<sup>1</sup>, P. de Laverny<sup>1</sup>, P. A. Palicio<sup>1</sup>, A. Spagna<sup>2</sup>, L. Spina<sup>3</sup>,
D. Katz<sup>4</sup>, P. Re Fiorentin<sup>2</sup>, E. Poggio<sup>1,2</sup>, P.J. McMillan<sup>5</sup>, A. Vallenari<sup>3</sup>, M.G. Lattanzi<sup>2,6</sup>, G.M. Seabroke<sup>7</sup>
         L. Casamiquela<sup>8,4</sup>, A. Bragaglia<sup>9</sup>, T. Antoja<sup>10</sup>, C. A. L. Bailer-Jones<sup>11</sup>, M. Schultheis<sup>1</sup>, R. Andrae<sup>11</sup>
M. Fouesneau<sup>11</sup>, M. Cropper<sup>7</sup>, T. Cantat-Gaudin<sup>10,11</sup>, A. Bijaoui<sup>1</sup>, U. Heiter<sup>12</sup>, A. G. A. Brown<sup>13</sup>, T. Prusti<sup>14</sup>,
          J.H.J. de Bruijne 14, F. Arenou 4, C. Babusiaux 15, 4, M. Biermann 16, O.L. Creevey 1, C. Ducourant 8,
          D.W. Evans<sup>17</sup>, L. Eyer<sup>18</sup>, R. Guerra<sup>19</sup>, A. Hutton<sup>20</sup>, C. Jordi<sup>10</sup>, S. A. Klioner<sup>21</sup>, U.L. Lammers<sup>19</sup>, L. Lindegren<sup>5</sup>, X. Luri<sup>10</sup>, F. Mignard<sup>1</sup>, C. Panem<sup>22</sup>, D. Pourbaix<sup>23,24,†</sup>, S. Randich<sup>25</sup>, P. Sartoretti<sup>4</sup>,
       C. Soubiran<sup>8</sup>, P. Tanga<sup>1</sup>, N. A. Walton<sup>17</sup>, U. Bastian<sup>16</sup>, R. Drimmel<sup>2</sup>, F. Jansen<sup>26</sup>, **, F. van Leeuwen<sup>17</sup>,
       J. Bakker<sup>19</sup>, C. Cacciari<sup>9</sup>, J. Castañeda<sup>27</sup>, F. De Angeli<sup>17</sup>, C. Fabricius<sup>10</sup>, Y. Frémat<sup>28</sup>, L. Galluccio<sup>1</sup>,
     A. Guerrier<sup>22</sup>, E. Masana<sup>10</sup>, R. Messineo<sup>29</sup>, N. Mowlavi<sup>18</sup>, C. Nicolas<sup>22</sup>, K. Nienartowicz<sup>30,31</sup>, F. Pailler<sup>22</sup>
 P. Panuzzo<sup>4</sup>, F. Riclet<sup>22</sup>, W. Roux<sup>22</sup>, R. Sordo<sup>3</sup>, F. Thévenin<sup>1</sup>, G. Gracia-Abril<sup>32,16</sup>, J. Portell<sup>10</sup>, D. Teyssier<sup>33</sup>
 M. Altmann<sup>16,34</sup>, M. Audard<sup>18,31</sup>, I. Bellas-Velidis<sup>35</sup>, K. Benson<sup>7</sup>, J. Berthier<sup>36</sup>, R. Blomme<sup>28</sup>, P. W. Burgess<sup>17</sup>,
            D. Busonero<sup>2</sup>, G. Busso<sup>17</sup>, H. Cánovas<sup>33</sup>, B. Carry<sup>1</sup>, A. Cellino<sup>2</sup>, N. Cheek<sup>37</sup>, G. Clementini<sup>9</sup>,
        Y. Damerdji<sup>38,39</sup>, M. Davidson<sup>40</sup>, P. de Teodoro<sup>19</sup>, M. Nuñez Campos<sup>20</sup>, L. Delchambre<sup>38</sup>, A. Dell'Oro<sup>25</sup>,
 P. Esquej<sup>41</sup>, J. Fernández-Hernández<sup>42</sup>, E. Fraile<sup>41</sup>, D. Garabato<sup>43</sup>, P. García-Lario<sup>19</sup>, E. Gosset<sup>38,24</sup>, R. Haigron<sup>4</sup>,
   J.-L. Halbwachs<sup>44</sup>, N.C. Hambly<sup>40</sup>, D.L. Harrison<sup>17,45</sup>, J. Hernández<sup>19</sup>, D. Hestroffer<sup>36</sup>, S.T. Hodgkin<sup>17</sup>,
B. Holl<sup>18,31</sup>, K. Janßen<sup>46</sup>, G. Jevardat de Fombelle<sup>18</sup>, S. Jordan<sup>16</sup>, A. Krone-Martins<sup>47,48</sup>, A.C. Lanzafame<sup>49,50</sup>
W. Löffler<sup>16</sup>, O. Marchal<sup>44</sup>, P.M. Marrese<sup>51,52</sup>, A. Moitinho<sup>47</sup>, K. Muinonen<sup>53,54</sup>, P. Osborne<sup>17</sup>, E. Pancino<sup>25,52</sup>,
T. Pauwels<sup>28</sup>, C. Reyle<sup>55</sup>, M. Riello<sup>17</sup>, L. Rimoldini<sup>31</sup>, T. Roegiers<sup>56</sup>, J. Rybizki<sup>11</sup>, L. M. Sarro<sup>57</sup>, C. Siopis<sup>23</sup>,
     M. Smith<sup>7</sup>, A. Sozzetti<sup>2</sup>, E. Utrilla<sup>20</sup>, M. van Leeuwen<sup>17</sup>, U. Abbas<sup>2</sup>, P. Ábrahám<sup>58,59</sup>, A. Abreu Aramburu<sup>42</sup>,
    C. Aerts<sup>60,61,11</sup>, J.J. Aguado<sup>57</sup>, M. Ajaj<sup>4</sup>, F. Aldea-Montero<sup>19</sup>, G. Altavilla<sup>51,52</sup>, M. A. Álvarez<sup>43</sup>, J. Alves<sup>62</sup>.
         F. Anders<sup>10</sup>, R. I. Anderson<sup>63</sup>, E. Anglada Varela<sup>42</sup>, D. Baines<sup>33</sup>, S. G. Baker<sup>7</sup>, L. Balaguer-Núñez<sup>10</sup>,
    E. Balbinot<sup>64</sup>, Z. Balog<sup>16,11</sup>, C. Barache<sup>34</sup>, D. Barbato<sup>18,2</sup>, M. Barros<sup>47</sup>, M. A. Barstow<sup>65</sup>, S. Bartolomé<sup>10</sup>
  J.-L. Bassilana<sup>66</sup>, N. Bauchet<sup>4</sup>, U. Becciani<sup>49</sup>, M. Bellazzini<sup>9</sup>, A. Berihuete<sup>67</sup>, M. Bernet<sup>10</sup>, S. Bertone<sup>68,69,2</sup>,
             L. Bianchi<sup>70</sup>, A. Binnenfeld<sup>71</sup>, S. Blanco-Cuaresma<sup>72</sup>, T. Boch<sup>44</sup>, A. Bombrun<sup>73</sup>, D. Bossini<sup>74</sup>,
 S. Bouquillon<sup>34,75</sup>, L. Bramante<sup>29</sup>, E. Breedt<sup>17</sup>, A. Bressan<sup>76</sup>, N. Brouillet<sup>8</sup>, E. Brugaletta<sup>49</sup>, B. Bucciarelli<sup>2,6</sup>
        A. Burlacu<sup>77</sup>, A. G. Butkevich<sup>2</sup>, R. Buzzi<sup>2</sup>, E. Caffau<sup>4</sup>, R. Cancelliere<sup>78</sup>, R. Carballo<sup>79</sup>, T. Carlucci<sup>34</sup>,
            M.I. Carnerero<sup>2</sup>, J.M. Carrasco<sup>10</sup>, M. Castellani<sup>51</sup>, A. Castro-Ginard<sup>13</sup>, L. Chaoul<sup>22</sup>, P. Charlot<sup>8</sup>
               L. Chemin<sup>80</sup>, V. Chiaramida<sup>29</sup>, A. Chiavassa<sup>1</sup>, N. Chornay<sup>17</sup>, G. Comoretto<sup>33,81</sup>, G. Contursi<sup>1</sup>,
 W. J. Cooper<sup>82,2</sup>, T. Cornez<sup>66</sup>, S. Cowell<sup>17</sup>, F. Crifo<sup>4</sup>, M. Crosta<sup>2,83</sup>, C. Crowley<sup>73</sup>, C. Dafonte<sup>43</sup>, A. Dapergolas<sup>35</sup>,
        P. David<sup>36</sup>, F. De Luise<sup>84</sup>, R. De March<sup>29</sup>, J. De Ridder<sup>60</sup>, R. de Souza<sup>85</sup>, A. de Torres<sup>73</sup>, E. F. del Peloso<sup>16</sup>,
  E. del Pozo<sup>20</sup>, M. Delbo<sup>1</sup>, A. Delgado<sup>41</sup>, J.-B. Delisle<sup>18</sup>, C. Demouchy<sup>86</sup>, T.E. Dharmawardena<sup>11</sup>, P. Di Matteo<sup>4</sup>,
 S. Diakite<sup>87</sup>, C. Diener<sup>17</sup>, E. Distefano<sup>49</sup>, C. Dolding<sup>7</sup>, B. Edvardsson<sup>88</sup>, H. Enke<sup>46</sup>, C. Fabre<sup>89</sup>, M. Fabrizio<sup>51,52</sup>,
 S. Faigler<sup>90</sup>, G. Fedorets<sup>53,91</sup>, P. Fernique<sup>44,92</sup>, F. Figueras<sup>10</sup>, Y. Fournier<sup>46</sup>, C. Fouron<sup>77</sup>, F. Fragkoudi<sup>93,94,95</sup>,
  M. Gai<sup>2</sup>, A. Garcia-Gutierrez<sup>10</sup>, M. Garcia-Reinaldos<sup>19</sup>, M. García-Torres<sup>96</sup>, A. Garofalo<sup>9</sup>, A. Gavel<sup>12</sup>, P. Gavras<sup>41</sup>, E. Gerlach<sup>21</sup>, R. Geyer<sup>21</sup>, P. Giacobbe<sup>2</sup>, G. Gilmore<sup>17</sup>, S. Girona<sup>97</sup>, G. Giuffrida<sup>51</sup>, R. Gomel<sup>90</sup>,
       A. Gomez<sup>43</sup>, J. González-Núñez<sup>37,98</sup>, I. González-Santamaría<sup>43</sup>, J. J. González-Vidal<sup>10</sup>, M. Granvik<sup>53,99</sup>
      P. Guillout<sup>44</sup>, J. Guiraud<sup>22</sup>, R. Gutiérrez-Sánchez<sup>33</sup>, L.P. Guy<sup>31,100</sup>, D. Hatzidimitriou<sup>101,35</sup>, M. Hauser<sup>11,102</sup>,
        M. Haywood<sup>4</sup>, A. Helmi<sup>64</sup>, M. H. Sarmiento<sup>20</sup>, S. L. Hidalgo<sup>103,104</sup>, N. Hładczuk<sup>19,105</sup>,
             D. Hobbs<sup>5</sup>, G. Holland<sup>17</sup>, H. E. Huckle<sup>7</sup>, K. Jardine<sup>106</sup>, G. Jasniewicz<sup>107</sup>, A. Jean-Antoine Piccolo<sup>22</sup>,
         Ó. Jiménez-Arranz<sup>10</sup>, J. Juaristi Campillo<sup>16</sup>, F. Julbe<sup>10</sup>, L. Karbevska<sup>31,108</sup>, P. Kervella<sup>109</sup>, S. Khanna<sup>64,2</sup>
      A. J. Korn<sup>12</sup>, Á. Kóspál<sup>58,11,59</sup>, Z. Kostrzewa-Rutkowska<sup>13,110</sup>, K. Kruszyńska<sup>111</sup>, M. Kun<sup>58</sup>, P. Laizeau<sup>112</sup>,
```

<sup>\*</sup> Corresponding author: A. Recio-Blanco, e-mail: arecio@oca.eu

<sup>\*\*</sup> Retired.

```
S. Lambert<sup>34</sup>, A.F. Lanza<sup>49</sup>, Y. Lasne<sup>66</sup>, J.-F. Le Campion<sup>8</sup>, Y. Lebreton<sup>109,113</sup>, T. Lebzelter<sup>62</sup>, S. Leccia<sup>114</sup>,
        N. Leclerc<sup>4</sup>, I. Lecoeur-Taibi<sup>31</sup>, S. Liao<sup>115,2,116</sup>, E.L. Licata<sup>2</sup>, H.E.P. Lindstrøm<sup>2,117,118</sup>, T.A. Lister<sup>119</sup>,
      E. Livanou<sup>101</sup>, A. Lobel<sup>28</sup>, A. Lorca<sup>20</sup>, C. Loup<sup>44</sup>, P. Madrero Pardo<sup>10</sup>, A. Magdaleno Romeo<sup>77</sup>, S. Managau<sup>66</sup>, R. G. Mann<sup>40</sup>, M. Manteiga<sup>120</sup>, J. M. Marchant<sup>121</sup>, M. Marconi<sup>114</sup>, J. Marcos<sup>33</sup>, M. M. S. Marcos Santos<sup>37</sup>,
   D. Marín Pina<sup>10</sup>, S. Marinoni<sup>51,52</sup>, F. Marocco<sup>122</sup>, D.J. Marshall<sup>123</sup>, L. Martin Polo<sup>37</sup>, J.M. Martín-Fleitas<sup>20</sup>
     G. Marton<sup>58</sup>, N. Mary<sup>66</sup>, A. Masip<sup>10</sup>, D. Massari<sup>9</sup>, A. Mastrobuono-Battisti<sup>4</sup>, T. Mazeh<sup>90</sup>, S. Messina<sup>49</sup>,
     D. Michalik<sup>14</sup>, N. R. Millar<sup>17</sup>, A. Mints<sup>46</sup>, D. Molina<sup>10</sup>, R. Molinaro<sup>114</sup>, L. Molnár<sup>58,124,59</sup>, G. Monari<sup>44</sup>,
 M. Monguió<sup>10</sup>, P. Montegriffo<sup>9</sup>, A. Montero<sup>20</sup>, R. Mor<sup>10</sup>, A. Mora<sup>20</sup>, R. Morbidelli<sup>2</sup>, T. Morel<sup>38</sup>, D. Morris<sup>40</sup>,
   T. Muraveva<sup>9</sup>, C. P. Murphy<sup>19</sup>, I. Musella<sup>114</sup>, Z. Nagy<sup>58</sup>, L. Noval<sup>66</sup>, F. Ocaña<sup>33,125</sup>, A. Ogden<sup>17</sup>, C. Ordenovic<sup>1</sup>,
                   J.O. Osinde<sup>41</sup>, C. Pagani<sup>65</sup>, I. Pagano<sup>49</sup>, L. Palaversa<sup>126,17</sup>, L. Pallas-Quintela<sup>43</sup>, A. Panahi<sup>90</sup>,
       S. Payne-Wardenaar<sup>16</sup>, X. Peñalosa Esteller<sup>10</sup>, A. Penttilä<sup>53</sup>, B. Pichon<sup>1</sup>, A. M. Piersimoni<sup>84</sup>, F.-X. Pineau<sup>44</sup>
             E. Plachy<sup>58,124,59</sup>, G. Plum<sup>4</sup>, A. Prša<sup>127</sup>, L. Pulone<sup>51</sup>, E. Racero<sup>37,125</sup>, S. Ragaini<sup>9</sup>, M. Rainer<sup>25,128</sup>,
     C.M. Raiteri<sup>2</sup>, P. Ramos<sup>10,44</sup>, M. Ramos-Lerate<sup>33</sup>, S. Regibo<sup>60</sup>, P.J. Richards<sup>129</sup>, C. Rios Diaz<sup>41</sup>, V. Ripepi<sup>114</sup>, A. Riva<sup>2</sup>, H.-W. Rix<sup>11</sup>, G. Rixon<sup>17</sup>, N. Robichon<sup>4</sup>, A.C. Robin<sup>55</sup>, C. Robin<sup>66</sup>, M. Roelens<sup>18</sup>,
             H.R.O. Rogues<sup>86</sup>, L. Rohrbasser<sup>31</sup>, M. Romero-Gómez<sup>10</sup>, N. Rowell<sup>40</sup>, F. Royer<sup>4</sup>, D. Ruz Mieres<sup>17</sup>
K. A. Rybicki<sup>111</sup>, G. Sadowski<sup>23</sup>, A. Sáez Núñez<sup>10</sup>, A. Sagristà Sellés<sup>16</sup>, J. Sahlmann<sup>41</sup>, E. Salguero<sup>42</sup>, N. Samaras<sup>28,130</sup>, V. Sanchez Gimenez<sup>10</sup>, N. Sanna<sup>25</sup>, R. Santoveña<sup>43</sup>, M. Sarasso<sup>2</sup>, E. Sciacca<sup>49</sup>, M. Segol<sup>86</sup>, J. C. Segovia<sup>37</sup>, D. Ségransan<sup>18</sup>, D. Semeux<sup>89</sup>, S. Shahaf<sup>131</sup>, H. I. Siddiqui<sup>132</sup>, A. Siebert<sup>44,92</sup>, L. Siltala<sup>53</sup>,
       A. Silvelo<sup>43</sup>, E. Slezak<sup>1</sup>, I. Slezak<sup>1</sup>, R. L. Smart<sup>2</sup>, O. N. Snaith<sup>4</sup>, E. Solano<sup>133</sup>, F. Solitro<sup>29</sup>, D. Souami<sup>109,134</sup>,
                J. Souchay<sup>34</sup>, F. Spoto<sup>72</sup>, I.A. Steele<sup>121</sup>, H. Steidelmüller<sup>21</sup>, C.A. Stephenson<sup>33,135</sup>, M. Süveges<sup>136</sup>
     J. Surdej<sup>38,137</sup>, L. Szabados<sup>58</sup>, E. Szegedi-Elek<sup>58</sup>, F. Taris<sup>34</sup>, M. B. Taylor<sup>138</sup>, R. Teixeira<sup>85</sup>, L. Tolomei<sup>29</sup>,
 N. Tonello<sup>97</sup>, F. Torra<sup>27</sup>, J. Torra<sup>10,†</sup>, G. Torralba Elipe<sup>43</sup>, M. Trabucchi<sup>139,18</sup>, A. T. Tsounis<sup>140</sup>, C. Turon<sup>4</sup>, A. Ulla<sup>141</sup>, N. Unger<sup>18</sup>, M. V. Vaillant<sup>66</sup>, E. van Dillen<sup>86</sup>, W. van Reeven<sup>142</sup>, O. Vanel<sup>4</sup>, A. Vecchiato<sup>2</sup>, Y. Viala<sup>4</sup>, D. Vicente<sup>97</sup>, S. Voutsinas<sup>40</sup>, M. Weiler<sup>10</sup>, T. Wevers<sup>17,143</sup>, Ł. Wyrzykowski<sup>111</sup>, A. Yoldas<sup>17</sup>, P. Yvard<sup>86</sup>,
                                                                     H. Zhao<sup>1</sup>, J. Zorec<sup>144</sup>, S. Zucker<sup>71</sup>, T. Zwitter<sup>145</sup>
```

(Affiliations can be found after the references)

Received 9 March 2022 / Accepted 25 May 2022

#### **ABSTRACT**

Context. The motion of stars has been used to reveal details of the complex history of the Milky Way, in constant interaction with its environment. Nevertheless, to reconstruct the Galactic history puzzle in its entirety, the chemo-physical characterisation of stars is essential. Previous Gaia data releases were supported by a smaller, heterogeneous, and spatially biased mixture of chemical data from ground-based observations.

Aims. Gaia Data Release 3 opens a new era of all-sky spectral analysis of stellar populations thanks to the nearly 5.6 million stars observed by the Radial Velocity Spectrometer (RVS) and parametrised by the GSP-Spec module. In this work, we aim to demonstrate the scientific quality of

Gaia's Milky Way chemical cartography through a chemo-dynamical analysis of disc and halo populations.

Mathods, Stellar atmospheric parameters and chemical abundances provided by Gaia DR3 spectroscopy are combined with Dl

Methods. Stellar atmospheric parameters and chemical abundances provided by Gaia DR3 spectroscopy are combined with DR3 radial velocities and EDR3 astrometry to analyse the relationships between chemistry and Milky Way structure, stellar kinematics, and orbital parameters.

Results. The all-sky Gaia chemical cartography allows a powerful and precise chemo-dynamical view of the Milky Way with unprecedented spatial coverage and statistical robustness. First, it reveals the strong vertical symmetry of the Galaxy and the flared structure of the disc. Second, the observed kinematic disturbances of the disc – seen as phase space correlations – and kinematic or orbital substructures are associated with chemical patterns that favour stars with enhanced metallicities and lower  $[\alpha/Fe]$  abundance ratios compared to the median values in the radial distributions. This is detected both for young objects that trace the spiral arms and older populations. Several  $\alpha$ , iron-peak elements and at least one heavy element trace the thin and thick disc properties in the solar cylinder. Third, young disc stars show a recent chemical impoverishment in several elements. Fourth, the largest chemo-dynamical sample of open clusters analysed so far shows a steepening of the radial metallicity gradient with age, which is also observed in the young field population. Finally, the Gaia chemical data have the required coverage and precision to unveil galaxy accretion debris and heated disc stars on halo orbits through their  $[\alpha/Fe]$  ratio, and to allow the study of the chemo-dynamical properties of globular clusters.

Conclusions. Gaia DR3 chemo-dynamical diagnostics open new horizons before the era of ground-based wide-field spectroscopic surveys. They unveil a complex Milky Way that is the outcome of an eventful evolution, shaping it to the present day.

**Key words.** Galaxy: abundances – Galaxy: evolution – Galaxy: kinematics and dynamics – Galaxy: disk – Galaxy: halo

## 1. Introduction

The European Space Agency *Gaia* mission has transformed our understanding of the Milky Way, thanks to its ability to trace the motion of stars in the sky (Gaia Collaboration 2023a). The observation of these movements has allowed us to see the Galaxy as an evolving system. Components that were previously thought to be distinct (the thin disc in the Galactic plane with ongoing

star formation, the more diffuse and older thick disc, the central bulge, and the extended stellar halo) now appear to be interlinked formation phases of a system in clear interaction with its environment. In particular, studies of stellar orbits and kinematics have uncovered a considerable proportion of merger debris in the halo (e.g. Helmi et al. 2018; Belokurov et al. 2018; Malhan et al. 2018; Myeong et al. 2019; Helmi 2020, and references therein) and the Galactic disc (e.g. Sestito et al. 2020; Re Fiorentin et al. 2021). Additionally, investigations of stellar motions have

<sup>†</sup> Deceased.

revealed the Galactic disc phase mixing process, which is subsequent to a mildly disturbed state (Antoja et al. 2018). A massive disc-crossing perturber (e.g. Binney & Schönrich 2018) – possibly akin to the Sagittarius dwarf galaxy (Laporte et al. 2019a; Bland-Hawthorn et al. 2019) – or a strong buckling of the stellar bar (e.g. Khoperskov et al. 2020) are the most likely interpretations of this phenomenon. A recent or ongoing encounter with a satellite galaxy seems also to be responsible for the rapidly precessing disc warp (Poggio et al. 2020, 2021a). In summary, the picture of a 'living and breathing Galaxy' has emerged thanks to *Gaia* data (Belokurov 2019; Brown 2021).

Despite the above-mentioned transformational results, stellar motions alone do not allow a complete reconstruction of the intricate puzzle of Galactic history. The orbit of a star evolves in response to fluctuations in the Galaxy's gravitational field (e.g. Sellwood & Binney 2002). As a consequence, the reconstruction of the history of the Milky Way based on the interpretation of stellar motions in terms of evolutionary processes is hampered by degenerate explanations and the complex interplay of different physical mechanisms.

Indeed, understanding how galaxies like the Milky Way form and evolve remains a challenge. In the cold dark matter Universe, galaxies grow through a sequence of merger and accretion events. However, the impact of these events on the evolution of a galaxy is extremely difficult to predict because of the complex physics of baryons. As a consequence, studying the chemophysical properties of matter is essential to comprehend the Galaxy in which we live. Fortunately, we have a powerful tool at our disposal: stellar spectroscopy.

The study of stellar spectra gave rise to the science of astrophysics in the 19th century (e.g. Huggins & Miller 1864; Huggins & Huggins 1899) and, since then, the varying characteristics of spectral absorption lines have been used by researchers to decipher the physical properties of stars (Maury & Pickering 1897; Cannon & Pickering 1918). Stellar parametrisation became a powerful decryption tool, allowing us to unveil the chemical composition of stellar atmospheres (Payne 1925a,b), and to provide observational evidence of the stellar nucleosynthesis theory (Burbidge et al. 1957). Stars form during the collapse of molecular clouds of gas and dust. Like alchemists, stars of different masses synthesise all chemical elements except hydrogen<sup>1</sup>; they partially return them in the later stages of their life into the interstellar medium, from which new stars are born. As a consequence, the stellar chemical composition evolves from one generation to the next, and reflects the gas conditions at the time and place of the formation of a star. Moreover, contrary to stellar motions, the chemical abundances of a star's atmosphere are conserved<sup>2</sup> from its birth, and can therefore be used to trace its origin. Chemical abundances break degenerated dynamical scenarios with a variety of conserved parameters (e.g. they play a key role in merger debris studies; e.g. Helmi 2020). Therefore, stellar atmospheres record the past in their chemical abundances, allowing a look-back time that varies between a few hundred million years and the age of the first stars in the Universe.

In this framework, previous intermediate *Gaia* data releases had to be complemented with chemical data from ground-based observations. However, ground-based spectroscopic surveys like GALAH (e.g. Buder et al. 2021), APOGEE (Abdurro'uf et al. 2022), *Gaia*-ESO Survey (Gilmore et al. 2022; Randich et al.

2022), and RAVE (Steinmetz et al. 2020), despite the recent improvement of multiplex capabilities, are still hampered by spatially biased samples. In addition, the inhomogeneity induced by different analysis procedures, targeted stellar types, and spectral configurations blur the collected chemical information. Moreover, ground-based spectroscopy suffers from time-dependent effects such as the Earth's atmospheric absorption and instrumental systematic effects, which are difficult to model with discontinuous data collections.

Fortunately, the context is now evolving favourably. Gaia Data Release 3 (DR3; Gaia Collaboration 2023c) opens a new era of all-sky spectroscopy and chemo-physical characterisation of Galactic stellar populations, and includes a new transformational data set that confirms Gaia's leading role in the golden age of Galactic archaeology: the largest homogeneous spectral analysis performed so far with a total of 5 594 205 stars observed by the Radial Velocity Spectrometer (RVS; Cropper et al. 2018; Katz et al. 2023) and parametrised by the General Stellar Parametriser - spectroscopy (GSP-Spec; Recio-Blanco et al. 2023). With continuous data collection for 34 months outside the Earth's atmosphere, and a large volume coverage reaching distances of about 8 kpc from the Sun (thanks to the population of giant stars), the Gaia DR3 spectroscopic survey provides stellar parameters and chemical abundances in all major Galactic populations, sharpening our global view of the Milky Way. In addition to the sky coverage advantage, it is worth comparing this Gaia DR3 GSP-Spec catalogue with high-resolution ground-based surveys in other crucial characteristics for Milky Way studies, as the number of analysed stars, the limiting magnitude, and the explored chemical diagnostics. For magnitudes brighter than  $G = 13.6^3$ , there are more stars in the Gaia DR3 GSP-Spec catalogue than in any other groundbased survey (with both GALAH and APOGEE representing only ~8% of Gaia GSP-Spec). For magnitudes fainter than 13.6, Gaia GSP-Spec has about 61 000 stars (reaching G = 16.1 mag), GALAH has about 130 000 stars (20% of the survey, reaching G = 18 mag) and APOGEE about 314 000 stars (43% of the survey, reaching  $G \simeq 20$  mag). Concerning the nucleosynthesis diagnostics<sup>4</sup> through individual abundance estimates, Gaia DR3 GSP-Spec explores five different nucleosynthetic channels with 13 chemical elements, while GALAH covers seven nucleosynthetic channels with 21 elements, and APOGEE six channels with 24 elements.

The goal of this paper is to demonstrate the scientific quality of *Gaia*'s chemical cartography through a chemo-dynamical analysis of disc and halo populations. To this purpose, Sect. 2 presents the data that are used, including (i) DR3 atmospheric parameters and chemical abundances (Sect. 2.1), (ii) DR3 radial velocities (Sect. 2.2), (iii) EDR3 astrometric data and distances (Sect. 2.3), (iv) a set of stellar velocities and orbits specifically derived for this work (Sect. 2.4), and (v) the definition of working subsamples (Sect. 2.5) allowing us to optimise the scientific analysis, and illustrating the use of quality flags defined in Recio-Blanco et al. (2023).

In Sect. 3 we present the global chemical properties of the Milky Way through sky and Galactic maps (Sect. 3.1) and explore selection function effects (Sect. 3.2). Section 4

<sup>&</sup>lt;sup>1</sup> More particularly, the Big Bang nucleosynthesis produced H, He and Li, cosmic rays contribute to Li, Be and B production and stellar nucleosynthesis concerns all chemical elements except H.

<sup>&</sup>lt;sup>2</sup> With the exception of some chemical species whose surface abundance can be modified in certain stellar evolution phases.

<sup>&</sup>lt;sup>3</sup> In DR3, 99% of the GSP-Spec catalogue has Gmag < 13.6. This will strongly evolve in future releases, reaching much fainter magnitudes thanks to the continuous and on-going *Gaia* observations.

<sup>&</sup>lt;sup>4</sup> The following general nucleosynthetic channels are considered: (i) cosmic rays spallation, (ii) nuclear burning in low- and intermediate-mass stars, (iii) α-process in core collapse supernovae (massive stars), (iv) neutrino process in core collapse supernovae, (v) explosions of Type Ia supernovae (C+O white dwarfs in binary systems), (vi) slow neutron capture (s-process), and (vii) rapid neutron capture (r-process).

presents the radial and vertical chemical gradients of field stellar populations. In Sect. 5 we present our analysis of large-scale chemo-kinematical correlations, while in Sect. 6 we explore the relation between the orbital parameters and stellar chemistry. Subsequently, Sect. 7 is dedicated to chemo-dynamical relations in solar cylinder populations using individual element abundances, and in Sect. 8 we use the open clusters population to study chemo-kinematical correlations and the temporal evolution of disc radial chemical gradients.

Finally, Sect. 9 summarises the results of our Galactic chemo-dynamical analysis using the *Gaia* RVS GSP-Spec database. In particular, we discuss the observed chemical markers of Milky Way structure (Sect. 9.1), disc kinematic disturbances (Sect. 9.2), and satellite accretion (Sect. 9.3). This is completed with the examination of the detected chemodynamical trends of the last billion years (Sect. 9.4) and, finally, with a discussion of the Sun's chemo-dynamical properties in the context of its Galactic environment (Sect. 9.5). Our overall conclusions are presented in Sect. 10.

#### 2. Data

## 2.1. Stellar atmospheric parameters and chemical data

This work makes use of the stellar physical parameters and chemical abundances derived from the *Gaia* RVS spectra by the GSP-Spec module and available through the *astrophysical\_parameters* table of *Gaia* DR3. It is worth mentioning that the present work does not use the global metallicity [M/H] derived from BPRP spectra by the General Stellar Parametrizer from Photometry (GSP-Phot) and published in the GaiaSource and AstrophysicalParameters tables (mh\_gspphot field). Although GSP-Phot metallicities are suitable for different scientific purposes, their application to large-scale Galactic chemodynamical studies requires a calibration that at the time of writing this paper was not available.

GSP-Spec estimates the main atmospheric parameters (effective temperature  $T_{\text{eff}}$ , stellar surface gravity  $\log(g)^5$ , global metallicity  $[M/H]^6$ , and the global abundance of  $\alpha$ -elements with respect to iron  $[\alpha/\text{Fe}]$ ), together with the individual abundances of 12 different chemical elements from RVS spectra of single stars. The RVS wavelength range is [845 - 872] nm, and its medium resolving power is  $R = \lambda/\Delta\lambda \sim 11\,500$  (Cropper et al. 2018). This spectral parametrisation is based on the MatisseGauguin GSP-Spec workflow and is described in detail in the GSP-Spec processing paper (Recio-Blanco et al. 2023). It is worth recalling that the GSP-Spec [M/H] estimation considers all the non- $\alpha$  metallicity indicators in the observed spectra thanks to a four-dimensional synthetic spectra grid including not only the [M/H] dimension but also the  $[\alpha/\text{Fe}]$  one. Non- $\alpha$  indicators are dominated by Fe lines in the RVS domain. As a consequence, the estimated [M/H] value follows the [Fe/H] abundance with a tight correlation.

In the following sections,  $T_{\rm eff}$  is taken from the teff\_teff\_gspspec field;  $\log(g)$  comes from the logg\_gspspec field; [M/H] is taken from mh\_gspspec; and  $[\alpha/Fe]$  corresponds to alphafe\_gspspec with a calibration imposed that requires a zero average value for  $[\alpha/Fe]$  in the solar neighbourhood for any gravity (see Recio-Blanco et al. 2023, Table 4).

In a similar way, all the stellar individual chemical abundances come from the GSP-Spec estimates. In par-

ticular, this paper makes use of [N/Fe] (nfe\_gspspec), (mgfe\_gspspec), [Mg/Fe] [Si/Fe] (sife\_gspspec), [S/Fe] (sfe\_gspspec), [Ca/Fe] (cafe\_gspspec), [Ti/Fe] (tife\_gspspec), [Cr/Fe] (crfe\_gspspec), [Fe/M] (fem\_gspspec), [Ni/Fe] (nife\_gspspec), and [Ce/Fe] (cefe\_gspspec). As for the  $[\alpha/Fe]$  estimates, these individual abundances were calibrated following the prescriptions indicated in Table 4 of Recio-Blanco et al. (2023). It is important to note here that GSP-spec assumes the reference solar abundances of Grevesse et al. (2007).

In addition, we make use of the GSP-Spec quality flags reported in the flags\_gspspec string chain (which consists of 41 characters) defined in Recio-Blanco et al. (2023). For example, we make use of the first three characters in this chain (that is, flags\_gspspec[0], flags\_gspspec[1], and flags\_gspspec[2], reporting on the degree of parameter biases from line broadening) and called vbroadT, vbroadG, and vbroadM, respectively (see naming convention in Recio-Blanco et al. 2023).

Finally, the uncertainty on any derived parameter (Param\_unc) or abundance ([X/Fe]\_unc) is defined as half of the difference between its upper and lower confidence levels (e.g. Teff\_unc = [teff\_gspspec\_upper - teff\_gspspec\_lower]/2).

#### 2.2. Radial velocities

The complete GSP-Spec sample contains 5 594 205 stars in total (based on the query flags\_gspspec is not null). DR3 provides radial velocities (radial\_velocity,  $V_{Rad}$ ) for 33 834 834 stars (Katz et al. 2023) through the gaia\_source table. The GSP-Spec sample is a subset of the  $V_{\rm Rad}$  sample because the GSP-Spec sample was selected based on the signal-to-noise ratio (S/N) of the mean RVS spectra. An unpublished GSP-Spec S/N > 20 was used (Recio-Blanco et al. 2023). This was found to be very similar to rv\_expected\_sig\_to\_noise<sup>9</sup> in the *gaia\_source* table.  $V_{\rm Rad}$  is used to Doppler shift RVS CCD spectra to rest before combining them into a mean RVS spectrum (Seabroke et al., in prep.). The sensitivity of GSP-Spec parametrisation to spectra that are not perfectly corrected for their radial velocity shift is flagged in the GSP-Spec flags\_gspspec string. In particular, characters 3 to 5 (flags\_gspspec[3], flags\_gspspec[4] and flags\_gspspec[5]), called vradT, vradG, and vradM respectively, report on the degree of parameter biases from  $V_{\rm Rad}$ uncertainties (see Recio-Blanco et al. 2023, for more details on these flags).

## 2.3. Astrometric data and distances

High-precision astrometric parameters  $(\alpha, \delta, \mu_{\alpha*}, \mu_{\delta}, \varpi)$  from Gaia EDR3 (Gaia Collaboration 2021a) complement the above-described radial velocities, allowing three-dimensional study of stellar velocity. Thanks to the bright magnitude limit of the spectroscopic sample, the median parallax uncertainty is better than 20  $\mu$ as for most of our targets and the median uncertainty increases up to a maximum of ~40  $\mu$ as for the faintest stars with magnitude  $G \simeq 14$ .

Based on these *Gaia* EDR3 astrometric data, Bailer-Jones et al. (2021) geometric distances,  $r_{\text{Geo}}$ , are adopted in this study. To test the implications on our analysis of the Galaxy prior (a 3D model of the stellar distribution and extinction) adopted by Bailer-Jones et al. (2021), we defined an

<sup>&</sup>lt;sup>5</sup> g being expressed in cm.s<sup>-2</sup>.

<sup>&</sup>lt;sup>6</sup> We adopt the standard abundance notation for a given element *X*:  $[X/H] = \log(X/H)_{\star} - \log(X/H)_{\odot}$ , where (X/H) is the abundance by number, and  $\log \epsilon(X) \equiv \log(X/H) + 12$ .

 $<sup>^{7}</sup>$  α-elements are O, Ne, Mg, Si, S, Ar, Ca, and Ti.

<sup>&</sup>lt;sup>8</sup> It is important to note that *Gaia* DR3 catalogue values are not calibrated.

<sup>&</sup>lt;sup>9</sup> rvs\_expected\_sig\_to\_noise propagates median noise properties, whereas rvs\_spec\_sig\_to\_noise calculates the noise from the scatter on the signal in each wavelength bin and provides the median of these.